

Title: Contrail coverage over the United States of America during 2001 derived from AVHRR data

Corresponding author: Patrick Minnis      p.minnis@nasa.gov

Institution: Atmospheric Sciences, NASA Langley Research Center

Mailing address MS 420  
NASA Langley Research Center  
Hampton, VA 23681-2199 USA

First author: Rabindra Palikonda      r.palikonda@larc.nasa.gov

Third author: David P. Duda      d.p.duda@larc.nas.gov

Fourth author: Hermann Mannstein      hermann.mannstein@dlr.de

# Contrail coverage over the United States of America during 2001 derived from AVHRR data

Rabindra Palikonda

*Analytical Sciences and Materials, Inc., Hampton, Virginia, USA*

Patrick Minnis<sup>1</sup>,

*Atmospheric Sciences, NASA Langley Research Center, Hampton, Virginia, USA*

David P. Duda

*Hampton University, Hampton, Virginia, USA*

Hermann Mannstein

*DLR Institut für Physik der Atmosphäre, Oberpfaffenhofen, Wessling, Germany*

*Keywords:* contrails, aircraft emission, remote sensing, cirrus clouds

## **Abstract**

Linear contrail coverage, optical depth, and longwave radiative forcing are derived from *NOAA-15* and *NOAA-16* Advanced Very High Resolution Radiometer data taken during daytime over the United States of America (USA), southern Canada, and the adjacent oceans. Analyses were performed for all available overpasses during 2001, but were limited to the eastern half of the domain for *NOAA-15*. Contrail coverage averaged 1.17% and 0.66% from *NOAA-15* and 16, respectively, with an estimated combined maximum coverage during February of  $\sim 1.05\%$  and an August minimum of 0.57%. Mean optical depths varied by  $\sim 20\%$  with winter minima and summer maxima. The annual mean optical depth of 0.27 translated to a normalized contrail longwave radiative forcing of  $15.5 \text{ Wm}^{-2}$ . The overall daytime longwave radiative forcing for the domain is  $0.11 \text{ Wm}^{-2}$ . The normalized radiative forcing peaked during summer while the overall forcing was a maximum during winter because of the greater contrail coverage. A detailed error analysis showed that the linear contrail coverage was overestimated by  $\sim 40\%$  for both satellites. Errors in the mean *NOAA-15* optical depths and radiative forcing were negligible while their *NOAA-16* counterparts were overestimated

---

<sup>1</sup> *Corresponding author:* Patrick Minnis, MS 420, NASA Langley Research Center, Hampton, VA, USA 23681. Email: p.minnis@nasa.gov

by approximately 13%. Contrail coverage was dramatically lower than expected from previous studies, but could be the result of significantly decreased humidity. Contrail optical depths are much greater than theoretical estimates for the USA and empirical retrievals over Europe. The morning-afternoon difference in contrail coverage is hypothesized to be the result of saturation effects due to heavy morning air traffic and a possible diurnal cycle in upper-level humidity. Further modelling studies and additional satellite analyses are needed to explain the differences between the present results and previous studies and to better understand the effects of upper tropospheric humidity variability and saturation by heavy air traffic.

### **Zusammenfassung**

Zungenkondensstreifen-Einschluss, optische Tiefe, und das longwave Strahlungszwängen werden aus *NOAA-15* und *NOAA-16* Advanced Very High Resolution Radiometer Daten genommen während der Tageszeit über die Vereinigten Staaten von Nordamerika (USA), das südliche Kanada, und die angrenzenden Ozeane abgeleitet. Analysen wurden für alle vorhandenen Überführungen während 2001 durchgeführt, aber wurden auf die Osthälfte des Gebiets für *NOAA-15* beschränkt. Kondensstreifen-Einschluss nahm 1.17 % und 0.66 % von *NOAA-15* und *16*, beziehungsweise, mit einem geschätzten vereinigten maximalen Einschluss während des Februars von ~1.05 % und einem Minimum im August von 0.57 % den Durchschnitt. Bedeuten Sie optische Tiefen geändert durch ~20 % mit Winterminima und Sommermaxima. Die jährliche optische Mitteltiefe 0.27 übersetzt zu einem normalisierten Kondensstreifen longwave das Strahlungszwängen von 15.5 Wm<sup>-2</sup>. Die gesamte Tageszeit longwave das Strahlungszwängen für das Gebiet ist 0.11 Wm<sup>-2</sup>. Das normalisierte Strahlungszwängen kulminierte während des Sommers, während das gesamte Zwängen ein Maximum während des Winters wegen des größeren Kondensstreifen-Einschlusses war. Eine ausführliche Fehlerbyte zeigte, dass der Zungenkondensstreifen-Einschluss um ~40 % für beide Satelliten überschätzt wurde. Fehler in den optischen NOAA-15 Mitteltiefen und dem Strahlungszwängen

waren unwesentlich, während ihre *NOAA-16* Seitenstücke um etwa 13 % überschätzt wurden. Kondensstreifen-Einschluss war drastisch niedriger als erwartet von früheren Studien, aber konnte das Ergebnis bedeutsam der verminderten Feuchtigkeit sein. Kondensstreifen optische Tiefen ist viel größer als theoretische Schätzungen für die USA und empirische Wiederauffindungen über Europa. Der Morgennachmittag-Unterschied im Kondensstreifen-Einschluss wird vorausgesetzt, um das Ergebnis von Sättigungswirkungen zum passenden schweren Morgenluftverkehr und einem möglichen täglichen Zyklus in der Feuchtigkeit des oberen Niveaus zu sein. Weiter ist das Modellieren von Studien und zusätzlichen Satellitenanalysen erforderlich, die Unterschiede zwischen den gegenwärtigen Ergebnissen und früheren Studien zu erklären und besser die Wirkungen der oberen tropospheric Feuchtigkeitsveränderlichkeit und Sättigung durch den schweren Luftverkehr zu verstehen.

## 1. Introduction

Contrails often lead to the development of additional cirrus clouds that can affect climate via the radiation budget. Evaluation of contrail coverage and optical properties is crucial for assessing the impact of current and future climatic effects of air traffic. Current estimates of contrail coverage over the United States of America (USA) have been based on a single *NOAA-16* (*N16*) afternoon overpass time for recent studies and at four times of day for 1993-94 data from two satellites with different sensitivities and detection errors (PALIKONDA ET AL. 1999). Approximately 25,000 flights cross portions of the USA each day at different times of day. The commercial flight activity begins in earnest around 0600 LT and continues at relatively constant high intensity prior fading shortly before local midnight (GARBER ET AL. 2004). Because spreading contrail lifetimes are generally less than 4-6 hours (DUDA et al. 2001; MINNIS et al., 2002), the atmosphere should be cleansed of most contrail coverage by the beginning of the next day. If it is assumed that the state of the upper troposphere is, on average, the same during the day, this daily cycle should be reflected in the contrail properties and coverage. Given the air traffic diurnal cycle, the amount of contrail coverage detected

during morning satellite overpasses should be the same as that from data taken during the afternoon. However, if a given air mass penetrated by a large number of flights over the course of the day, it is possible that the contrail coverage during the afternoon would be less than during the morning because the spreading and saturation of contrails formed earlier in the day might mask contrails formed during the afternoon or decrease the amount of available moisture such that contrail growth is stymied during the afternoon. To obtain a better assessment of the average contrail coverage over the USA and its diurnal variation, this study analyzes data taken during 2001 from *NOAA-15 (N15)* in the early morning and from *N16* during the afternoon.

## 2. Data and methodology

The satellite data used for this study consist of 1-km radiances from the morning (~0730 LT) *N15* and mid-afternoon (~1430 LT) *N16* Advanced Very High Resolution Radiometer (AVHRR) passes over the continental USA covering the domain between 25°N and 55°N and 65°W and 130°W. The domain is divided into a 30 x 65 1°-region grid. Images from all available overpasses are analyzed to calculate the contrail statistics, however, only data taken at viewing zenith angles less than 50° are used because contrail coverage tends to increase when data from greater viewing angles are considered (PALIKONDA et al., 1999). Monthly mean maps of the statistics are computed using only those regions having more than 90% of the expected number of pixels during a given overpass and having at least ten images each month. Domain averages are computed using all available pixels. The Monterrey, California receiving station consistently had bad data from the *N15* AVHRR resulting in the loss of many western regions in the statistics. In addition, many of the *N15* overpasses for January and October yielded corrupted data and are not included in the results.

The contrail mask used to classify a pixel as contrail or otherwise is the image processing algorithm of MANNSTEIN et al. (1999), which is based on the brightness temperature difference, BTD, between the AVHRR channels 4 (10.8  $\mu\text{m}$ ) and 5 (12.0  $\mu\text{m}$ ). The fractional contrail areal coverage  $f_c$

for each image is simply the number of contrail pixels divided by the total number of pixels within the domain between 25°N and 55°N and 65°W and 130°W. After contrail pixels are identified, the visible optical depth, and contrail longwave radiative forcing CLRF are computed in following steps.

Assuming a typical contrail temperature of  $T_{con} = 224\text{K}$  (MEYER et al. 2002), the contrail emissivity for a given pixel with an 11- $\mu\text{m}$  temperature  $T$  is

$$\varepsilon = \frac{\{B(T) - B(T_b)\}}{\{B(T_{con}) - B(T_b)\}}, \quad (1)$$

where  $B$  is the Planck function at 10.8- $\mu\text{m}$  and the background temperature  $T_b$  is computed from surrounding non-contrail pixels. The background radiance is calculated as the average radiance of all pixels at a distance of 2 pixels horizontally, vertically, or diagonally from a contrail pixel that are not adjacent to any other contrail pixels. The background pixels for a hypothetical pair of crossing contrails are shaded gray in Fig. 1. To ensure that the background pixels are below the contrail,  $T_b > T_c$ . Otherwise,  $T_b$  is invalid. If no pixels meeting these criteria are found, the mean background radiance, calculated for the all other contrail pixels within the local 10' grid box, is used.

The visible optical depth  $\tau$  for the contrails is derived from the emissivity using the parameterization of MINNIS et al (1993),

$$\varepsilon = 1 - \exp[ a (\tau / \mu)^b ], \quad (2)$$

which accounts for the infrared scattering. In (2),  $\mu$  is the cosine of the viewing zenith angle, and the coefficients,  $a = -0.458$  and  $b = 1.033$ , are for an axi-symmetrical 20- $\mu\text{m}$  hexagonal ice column. To minimize false detections, all contrails with  $\tau > 1$  were eliminated from the processing.

The contrail longwave (LW; 5 - 50  $\mu\text{m}$ ) radiative forcing is

$$CLRF = (Q_b - Q_c) f_c, \quad (3)$$

where  $Q_c$  and  $Q_b$  are the LW fluxes for contrails and the background respectively. Broadband LW fluxes are calculated from the 10.8- $\mu\text{m}$  radiances as described by MINNIS and SMITH (1998). The normalized  $CLRF$ ,  $NCLRF$ , is simply the difference,  $Q_b - Q_c$ .

### 3. Results

Figures 2–5 show the monthly distribution of contrail cover over the domain. During April, for the morning overpass ( $NI5$ , Fig 2a), maximum contrail coverage occurs over the southeastern states, off the coasts of Texas and Louisiana, and in northern Ohio. In the afternoon ( $NI6$ , Fig 2b), maximum coverage occurs over North Dakota, Nevada, Washington, northern Mexico, and adjacent Pacific Ocean, areas not available from  $NI5$ . The  $NI5$  maximum over the western Gulf of Mexico is still evident as a relative maximum in the  $NI6$  results. The domain averages are 1.29% and 0.71% in the morning and afternoon, respectively. These means include differing numbers of regions. The morning July contrail cover (Fig. 3a) peaks over Virginia, North Carolina, South Carolina, and New York. Minimum coverage occurs over Texas, Louisiana, Alabama, and Minnesota. The areal coverage is almost 70% less during the afternoon (Fig. 3b). A local maximum occurred along the Atlantic coast from Maryland to Florida, and off the coasts of Oregon, Washington, and British Columbia. These areas of maximum coverage are similar to those in the  $NI5$  retrievals. The substantial morning-afternoon difference in areal coverage persists in September (Fig. 4). During the morning (Fig. 4a), maximum contrail coverage exceeds 2% over southwestern Canada, Georgia, Pennsylvania, and east of Virginia. The extensive contrail minimum in the afternoon (Fig. 4b) is defined by a triangle extending from southern California to South Dakota and to the tip of Florida. Maximum coverage occurred over British Columbia, Oregon, New England, Quebec, and Lake Winnipeg. During the winter, in the morning (Fig. 5a), contrail cover exceeds 1.5% over the southeastern states and Gulf of Mexico, off the coast of Oregon and Washington. The afternoon coverage during December (Fig. 5b)

peaks over northern Virginia, West Virginia, Maryland, and Pennsylvania. Local maxima are seen over New Mexico, Wisconsin, and west of California.

When averaged over all 12 months, the distributions produce more distinct patterns (Fig. 6). The contrail coverage is concentrated over the eastern third of the USA during the morning (Fig. 6a) with maxima over Lake Erie, New York, Kentucky, Virginia, the Carolinas, and Florida. Relative maxima are also apparent over southern and northern portions of Canada with a relative minimum in between them. In addition to having less contrail coverage than seen in the morning, the pattern during the afternoon (Fig. 6b) is different. The relative maxima over the eastern USA occur off the coast of Florida and over New Jersey and Pennsylvania. Over the central USA, fewer contrails occur over Oklahoma while more are observed to the north. Over many areas, relative minima that are observed in the morning are replaced with relative maxima during the afternoon and vice versa. Maxima are also evident over Washington, Oregon, southwestern Arizona, and southeastern New Mexico, areas not observed with *N15*. A pronounced minimum occurs over the central Rocky Mountains. Relative maxima are also seen off the California coast and, during the morning and afternoon, east of Maine over New Brunswick, Canada.

The *N16* results, including the mean values for *OD*, *CLRF*, and *NCLRF*, are summarized in Table 1 for the entire domain. Monthly means for *OD* and *NCLRF* from the regions available from *N15* coverage are also listed in Table 1. Table 2 provides the monthly and annual mean contrail coverage for only those areas that are common to both *N15* and *N16* retrievals. The coverage during the afternoon peaks during the winter and is at a minimum during July, differing by a factor of 3 (Table 1). For the eastern USA, the afternoon seasonal variation is nearly the same as that for the entire USA in both phase and magnitude (Table 2). However, as expected from Figs 2 -6, the contrail coverage during the morning is nearly twice that observed in the afternoon and the seasonal cycle is much less apparent. The coverage in the morning is at a maximum during May and minimum during

August and September with a range of 0.46%. This range is less than the afternoon seasonal variation in both absolute and relative terms. The most variation between morning and afternoon is seen during summer months when the contrail coverage differs by a factor of 2 to 3.

Considering only the eastern half of the USA (Table 2), on average, the contrail coverage ranges from a minimum of 0.71% during August to a maximum of 1.07% in February. Between February and May, the mean varies by less than 0.08. Similarly, between July and September, it varies by only 0.03%. Thus, the periods of minima and maxima are broad and the actual extrema at a given time of day or in a given year could occur in months other than February and August. Given that the  $NI6$  mean for the eastern half of the USA in Table 2 is nearly identical to that for the entire domain in Table 1, the ratios of the combined values to the  $NI6$  values in Table 2 were multiplied by the  $NI6$  values of  $f_c$  in Table 1 to estimate the combined coverage for the entire domain. The missing  $NI5$  months were filled via linear interpolation. The results shown in the last column of Table 2 show the broad winter-spring maximum with a seasonal range of 0.48%.

The mean contrail optical depths in Table 1 also vary with season to some degree. The summer maxima are 20 - 30% greater than the February minima. The annual mean optical depths, computed with contrail coverage weighting, from  $NI6$  are 0.28 compared to 0.26 from  $NI5$ . This 12% difference is relatively consistent from month to month. The  $NI5$  and  $NI6$  monthly frequency distributions of contrail optical depth in Figure 7 are remarkably consistent. During all months,  $0.2 < OD \leq 0.4$  for more than 30% of the contrails. Thicker contrails were observed more frequently in summer than during the winter and spring.

The contrail radiative forcing (Table 1) in the morning was greatest during the summer months and at a minimum during February. In the afternoon, the maximum and minimum CLRF occurred during October and July, respectively. CLRF depends on both the contrail coverage and its background. The monthly mean NCLRF varies smoothly through the seasons for both satellites. In

the morning, NCLRF varies from  $11 \text{ Wm}^{-2}$  in February to  $19 \text{ Wm}^{-2}$  during August. During the afternoon, NCLRF varies from  $11 \text{ Wm}^{-2}$  in March to  $22 \text{ Wm}^{-2}$  during August indicating that the thermal contrast changed by more than a factor of 2 between winter and summer during the afternoon for the entire domain. Although the *N15* and *N16* cannot be compared directly because of differences in regional sampling, their  $f_c$ -weighted annual mean values are very similar, together averaging  $15.4 \text{ Wm}^{-2}$ .

## 4 Discussion

### 4.1 Error analysis

The differences in contrail coverage between the two satellites may be due, in part, to different sensitivities of channels 4 and 5 on the two AVHRRs. Each channel has a slightly different spectral response function and slightly different calibration. Small differences in each channel can translate to large differences in the BTD relative to the pixel-use threshold value. Visually, the BTD images from the two satellites are quite different when constructed using the same temperature range and contrast suggesting that the contrail retrievals would be different using the same methodology. Some insight into those differences might be gained by examining the errors for the two method.

The automated detection method (MANNSTEIN et al. 1999) is based on BTD values that produce a linear feature in the image. This assumption of linearity can cause both under- and overestimates of contrail coverage. Contrails do not always maintain linearity causing the technique to miss some them. Natural clouds, rivers, and coastlines can also produce linear features that can be mistaken as contrails. Additionally, some contrails can be missed because their signals are insufficient to be detected. The technique is also sensitive to background variations and to minor peculiarities in the relative calibrations of the AVHRR channels 4 and 5. Thus, it is essential to estimate the errors in the detection method for each satellite and region analyzed. PALIKONDA et al. (1999) roughly estimated that the error rate for applying the same methodology to AVHRR data from *NOAA-11* and *12* re-

sulted in a 25% overestimate of the USA contrail coverage. MEYER et al. (2002) developed more rigorous correction methods (e.g., false alarm rate, stationary artifacts, detection efficiency) for their *NOAA-14* AVHRR contrail analysis over Europe.

Here, a user-interactive computer program was applied in the same manner as described by MINNIS et al. (2004b) to evaluate the results for each satellite using 3 randomly selected days during 3 different months. In the program, the pixels identified as contrails are overlaid on the T4 and BTM images. The results are examined both objectively by comparing T4 and BTM values for the contrails with the surroundings and subjectively using contrast adjustment. Contrail pixels can be added or deleted based on the analyst's judgment. Results are stored as images with each pixel identified as non-contrail or remaining, deleted, or added contrail. The contrail properties are then computed for all three of the latter categories.

Table 3 summarizes the error analyses for the selected days for each month and satellite. In general, for these days,  $f_c$  appears to be overestimated by ~40%. For *N16*, the deleted fraction accounts for roughly 57% of the original contrail coverage compared to 46% for *N15*. The fraction added is slightly larger for *N16* but is only about 25% of the deleted amount. To quantify the overall impact of the error a correction factor,  $CF(f_c)$ , was computed by dividing the remaining and added contrails by the original contrail fraction. The value of  $CF(f_c)$  is remarkably consistent from one month to the next averaging 0.61 and 0.57 for *N15* and *N16*, respectively. Thus, the true linear contrail coverage is likely to be 40% less than the values in Tables 1 and 2. As indicated in Figure 8, however, the greatest reductions in contrail coverage were outside the USA boundaries in areas of light air traffic. These large negative errors can explain the unexpectedly large values of  $f_c$  in Canada north of 50°N. It is likely that the overestimate of contrail coverage within the USA is less than the 40% average for the entire domain.

The contrail optical depths for *N15* are nearly identical for the original and corrected contrail coverage, on average. The optical depths for the remaining *N16* contrails, however, are 11% smaller than the deleted mean value. In all cases, the added contrails are thinner, in the mean, than the original contrails. Overall, there appears to be no need to correct the *N15* optical depths, while the *N16* ODs should probably be reduced by ~13%. Similar correction factors were found for NCLRF. The contrail properties for the selected days appear to be representative of the entire dataset. In all cases,  $\tau$  and NCLRF are typically within less than 10% of their counterparts in Table 1. The correction factors indicate that the *N16* OD and NCLRF values in Table 1 should be equal to or slightly less than the *N15* values instead of being larger.

The error analysis was conducted without the optical depth restriction. For *N15*, 1.1% of the remaining and added contrails had  $OD > 1$  compared to 0.4% of the deleted pixels. Only 0.4% of the *N16* remaining and added contrails had  $OD > 1$ , while 0.6% of the deleted pixels were optically thick. Thus, the exclusion of  $OD > 1$  in the generation of the statistics had little impact on the results. Errors were also examined using only those pixels with viewing zenith angles exceeding  $50^\circ$ . At those higher viewing angles, 60-70% of the contrail pixels were false detections while roughly 10% were added. The net result is similar to the analysis of MEYER et al. (2002) who showed a doubling of the false alarm rate at high angles. It is also consistent with the viewing zenith angle dependence reported by PALIKONDA et al. (1999). The 40% overestimate for the current results is slightly greater than that reported by MINNIS et al. (2004b) who applied the same error analysis to *N16* data over an ocean background confirming that surface variability adds to false detections.

#### 4.2 Diurnal variation

The error analysis indicates that the contrail mask works essentially the same for both satellites. Enhancement of the *N16* BTD and T4 imagery during the error analyses did not reveal any sig-

nificantly obvious new contrails, relative to *N15*, that were not detected with the automated algorithm. The added fractional coverage was about the same for both. Thus, it is concluded that the morning-afternoon difference in coverage is not an artifact of the analyses, but, rather, a real phenomenon. MINNIS et al. (2003) found that contrail frequency observed from the surface over the USA peaked around 0800 LT (close to *N15* overpass time) and was ~25% less around 1430 LT (the *N16* overpass time). The difference in frequency is only half of the difference in coverage (Table 2). These differences occur despite the air traffic maximum extending from 0900 to 1600 LT (GARBER et al., 2004).

Perhaps, this diurnal variation is a result of the cruise-altitude layers being moister during early morning, so contrails are more easily observed and more likely to grow. When a layer of air has sufficient water vapor for contrail formation and spreading, part of the water vapor will be removed by the contrails. If the layer is rising, the relative humidity (RH) will increase as the day proceeds and the contrail should grow rapidly and possibly precipitate more because of the greater RH or the layer begins forming natural cirrus. If not permanently removed by precipitation, the water vapor will remain locked in the contrails until the layer sinks. At that point, contrails will no longer form in the layer anyway. With reduced humidity in the layer because of earlier flights, the contrails could be less likely to form and less likely to spread as much in the affected layer even if it is neither sinking or rising. Because air is rising and sinking at different locations throughout the day, this contrail “saturation” effect would only alter the contrail potential in areas of heavy air traffic where the layer ascent is minor. Also, in heavy air traffic, spreading contrails might also produce a non-uniform cirrus deck that can obscure contrails.

Another reason for the morning-afternoon difference may be due to diurnal variations in the upper tropospheric humidity (UTH). During months with significant convection, UTH may be greater in the morning from previous day's convection and least during the mid-afternoon prior to

deep convection. The morning-afternoon variation in  $f_c$  is greatest during June and July and least during December and February, when solar-driven convection is weakest. This hypothesis is difficult to assess given that the standard radiosonde launches at 1200 and 0000 UTC roughly correspond to the hours prior to the *N15* overpass and the hours when deep convection is well underway. While it could be examined with numerical weather analyses, the humidity variation is beyond the scope of this paper.

#### 4.3 Relative humidity effects

Two conditions are necessary for contrail formation: air traffic and suitable atmospheric conditions. The air traffic over the USA is relatively heavy with more than 4000 km of potential contrails (flights above 7 km) every day in a given  $1^\circ$  box (GARBER et al. 2004). Thus, the USA contrail coverage can be dominated by formation conditions. DUDA et al. (2004) estimated the frequency of potential contrail conditions over the USA using Rapid Update Cycle (RUC) model data. Their Figure 2 showing potential coverage results for September 2001 are very similar to the afternoon contrail coverage in Figure 4. Similar correspondence was also found for November (not shown). Overall, the RUC-based potential USA contrail frequency during 2001 peaked during April at 30% and dropped to a minimum of  $\sim 12\%$  during the summer months, nearly reaching a secondary peak in November followed by a decrease during December (Figure 4, DUDA et al. 2004). The sequence is very similar to the observed contrail variation in Table 1. The contrail coverage is considerably less than the potential because the contrails can only be detected when existing clouds do not obscure them and air-traffic coincides with the moisture. This consistency with contrail potential and the nearly identical morning-afternoon optical depths in Figure 7 support the validity of the retrievals.

Although the relative seasonal variations between 1993-94 and 2001 are nearly identical, Table 4 reveals that the contrail coverage is only half of that detected by PALIKONDA et al. (1999) from

1993-94 *NOAA-11* and *12* AVHRR data and calculated by SAUSEN et al. (1998) using 1992 air traffic densities and multiple years of meteorological data. The differences are even greater if the daytime sampling is corrected for the absence of nighttime coverage. Using data from GARBER et al. (2004), it was determined that the daytime averages should be multiplied by 0.71 to account for the diminished air traffic at night. The diurnally corrected results are also listed in Table 4. If the overestimate indicated by the error analysis is correct, then the means should probably be decreased by an additional 40%. This dramatic difference between the expected and observed linear contrail coverage is puzzling. Because the air traffic should have risen by more than 30% or more between 1992 and 2001 (e.g., MINNIS et al. 2004a), the contrail coverage also should have increased.

Part of the reduction may be due to overestimates in the *NOAA-11* and *NOAA-12* analyses, but decreased RH is also a likely reason. MINNIS et al. (2003) found a diminished frequency of persistent contrails over the USA during 1999 relative to 1993-94 that corresponded to a drop in UTH as indicated by the mean RH at 300 hPa from the National Center for Environmental Prediction (NCEP) reanalyses data. As seen in Figure 8, the UTH was 45.5% during 1993-94 and decreased to 39.4% during 2001, one of the lowest values during the 30-year period. Since RH is a crucial factor in the formation of contrails, a reduction in RH should result in reduction of contrail cover and frequency of occurrence. From correlations of mean cirrus cloudiness and UTH in areas without heavy air traffic, MINNIS ET AL. (2004a) found that cirrus coverage decreases by an average of 0.4%/U<sub>TH</sub>. Thus, the cirrus amount would have diminished by ~2.5% over the USA between 1993-94 and 2001 and would likely include a decrease in contrail coverage.

#### 4.3 Comparisons with other results

The phasing of the observed seasonal cycles in contrail coverage differs from the theoretical results of SAUSEN et al. (1998) in Table 2 and PONATER et al. (2002), but is consistent with the con-

trail frequency observations from surface observations (MINNIS et al. 2003). The seasonal range (200%) in  $f_c$  is only half of that (400%) observed from the surface and computed theoretically. This range difference decreases if only the *NI6* values are used.

The seasonal variation in *OD* is similar to that computed by PONATER et al. (2002) with a maximum during the summer. Additionally, the greater occurrence of optically thick contrails during summer (Table 1 and Figure 6) is consistent with the greater maximum contrail optical depth computed by PONATER ET AL. (2002). However, the theoretical winter minimum relative to the summer maximum is significantly less than the observations. On average, the observed *ODs* are twice the value of those computed theoretically and 2.5 times more than those found over Europe by MEYER et al. (2002). Part of the difference may be due to warmer contrails over the USA than over Europe (PONATER et al. 2002) allowing for more water vapor available for particle growth over the USA. The use of the same fixed contrail temperature over both locations could introduce an artificial difference if the USA contrails are actually warmer, on average, than those over Europe. Another source of discrepancies in the *OD* could be the differences in the contrail particle emissivity model and the particle sizes. The ice crystal diameter in (2) has a diameter of 20  $\mu\text{m}$  compared to the 34  $\mu\text{m}$  used by MEYER et al. (2002).

The CLRF values also are considerably larger than those derived by PONATER et al. (2002). Part of the difference is due to *OD* discrepancies. The remaining differences are likely a result of differences in the background temperatures and the diurnal cycle in contrail coverage that is not included here. NCLRF in Table 1 is  $\sim 3 \text{ Wm}^{-2}$  greater than the nighttime value computed by MEYER et al. (2002). Given the differences in *OD* and the greater surface temperatures during the daytime, a larger difference would be expected. However, MEYER et al. (2002) used a model calculation assuming a clear land surface while the result here used the actual background radiances to estimate the amount of forcing. Since contrails often occur with cirrus clouds and even within cirrus clouds, the

radiative forcing should be smaller than that for clear sky conditions. The mean NCLRF is roughly equal to the normalized net radiative forcing computed by MINNIS et al. (1999) suggesting that the previous result is slightly too large. According to the results of MINNIS et al. (1999), the NCLRF should be approximately 1.5 times greater than the net radiative forcing so that NCLRF in the previous study would be about  $23 \text{ Wm}^{-2}$  for the USA latitude band after accounting for the OD differences between the current and previous study. MINNIS et al. (1999) assumed random overlap between contrails and average cloud cover. The current results are probably lower because contrails occur more frequently with a cirrus background than the random overlap assumption. The background would affect both the longwave and shortwave fluxes, so it is not possible without an explicit evaluation of the shortwave impact to comment on the net radiative forcing for this dataset.

## **5 Concluding Remarks**

The results shown here confirm, for the most part, the relative seasonal variations in contrail coverage and optical depths. Over the USA, contrail coverage peaks during the large winter and spring and bottoms out during the late summer. Contrail optical depth is greatest during summer, approximately 20% larger than the winter minimum value. Uncertainties in the magnitudes of contrail coverage are large. The detail error assessment indicates that the automated contrail detection method overestimates contrail coverage by 40% from both satellites. Refinements in the algorithm are needed reduce this error. The contrail optical depths and normalized contrail radiative forcing are robust and relatively insensitive to the presence of falsely detected contrails. Their values are significantly larger than those found theoretically and from satellite analyses over Europe. Additional analyses are needed to help resolve some of the remaining large differences between the theoretical calculations and the observations. Until these discrepancies are understood, it will not be possible to determine conclusively if the current model estimates are sufficiently accurate for estimating contrail

climate effects or whether additional improvements are needed. While the contrail longwave radiative forcing has been estimated empirically, this study has not addressed the net radiative forcing. The shortwave radiative forcing is more difficult to estimate because of the large anisotropy in the radiation field and the solar zenith angle dependence of the albedo. Estimation of the net forcing will be addressed in future research.

Additional discrepancies between the total contrail coverage found here and previous empirical and theoretical calculations can be explained to some extent by interannual variations in UTH which can have a large impact on contrail frequency and coverage. If it can explain the differences found here remains an open question that, perhaps, could be answered by examining the interannual variability in multi-year modelling results and deriving contrail coverage over the USA for other years. A morning-afternoon diurnal cycle in contrail coverage that is not governed by air traffic was found; it is characterized by a decrease during the afternoon that is most significant during summer. It is hypothesized that this cycle is due to a saturation effect caused by morning air traffic and a diurnal variation in UTH. More detailed modelling will be needed to better quantify why it occurs and to account for it in estimating contrail effects.

## **Acknowledgments**

This research was supported by the NASA Pathfinder Program and the NASA Office of Earth Science Radiation Sciences Program.

## **References**

- DUDA, D. P., P. MINNIS, and L. NGUYEN, 2001: Estimates of cloud radiative forcing in contrail clusters using GOES imagery. - *J. Geophys. Res.*, **106**, 4927-4937.
- DUDA, D. P., P. MINNIS, P. K. COSTULIS, and R. PALIKONDA, 2004: CONUS contrail frequency from RUC and flight track data. - *Meteorol. Z.*, submitted.
- GARBER, D. P., P. MINNIS, and P. K. COSTULIS, 2004: A USA commercial flight track database for upper tropospheric aircraft emission studies. - *Meteorol. Z.*, submitted.

- MANNSTEIN, H., R. MEYER, and P. WENDLING, 1999: Operational detection of contrails from NOAA AVHRR data. - *Int. J. Remote Sens.*, **20**, 1641-1660.
- MEYER, R., H. MANNSTEIN, R. MEERKÖTTER, U. SCHUMANN, and P. WENDLING, 2002: Regional radiative forcing by line-shaped contrails derived from satellite data. - *J. Geophys. Res.*, **107**, D10 10.1029/2001JD000426.
- MINNIS, P. J. K. AYERS, M. L. NORDEEN, and S. WEAVER, 2003: Contrail frequency over the United States from surface observations. - *J. Climate*, **16**, 3447-3462.
- MINNIS, P., J.K. AYERS, R. PALIKONDA, and D. PHAN, 2004a: Contrails, cirrus trends, and climate. - *J. Climate*, **17**, 1671-1685.
- MINNIS, P., L. NGUYEN, D. P. DUDA, and R. PALIKONDA, 2002: Spreading of isolated contrails during the 2001 air traffic shutdown. *10<sup>th</sup> AMS Conf. Aviation, range, and Aerospace Meteorol.*, Portland, OR, May 13-16, 33-36.
- MINNIS, P., R. PALIKONDA, B. J. WALTER, J. K. AYERS, and H. MANNSTEIN, 2004b: Contrail coverage over the North Pacific from AVHRR data. - *Meteorol. Z.*, submitted.
- MINNIS, P., U. SCHUMANN, D. R. DOELLING, K. M. GIERENS, and D. W. FAHEY, 1999: Global distribution of contrail radiative forcing. -- *Geophys. Res. Lett.*, **26**, 1853-1856.
- MINNIS, P. and W. L. SMITH, JR., 1998: Cloud and radiative fields derived from GOES-8 during SUCCESS and the ARM-UAV Spring 1996 Flight Series. - *Geophys. Res. Lett.*, **25**, 1113-1116.
- MINNIS, P., Y. TAKANO, and K.-N. LIOU, 1993: Inference of cirrus cloud properties using satellite-observed visible and infrared radiances, Part I: Parameterization of radiance fields. - *J. Atmos. Sci.*, **50**, 1279-1304.
- PALIKONDA, R., P. MINNIS, D. R. DOELLING, P. W. HECK, D. P. DUDA, H. MANNSTEIN, and U. SCHUMANN: Potential radiative impact of contrail coverage over continental USA estimated from AVHRR data. *Proc. AMS 10<sup>th</sup> Conf. Atmos. Rad.*, Madison, WI, June 28 – July 2, 181-184.
- PONATER, M., S. MARQUART, and R. SAUSEN, 2002: Contrails in a comprehensive global climate model: parameterisation and radiative forcing results. - *J. Geophys. Res.*, **107**, 10.1029/2001JD000429.
- SAUSEN, R., K. GIERENS, M. PONATER, M. and U. SCHUMANN, 1998: A diagnostic study of the global coverage by contrails, part I, present day climate. - *Theor. Appl. Climatol.* **61**, 127-141.

Table 1. NOAA-16 contrail properties for entire domain and NOAA-15 contrail properties for limited domain, 2001.

Month	N16 contrail cover (%)	N16 <i>OD</i>	N16 CLRF ( $\text{Wm}^{-2}$ )	N16 NCLRF ( $\text{Wm}^{-2}$ )	N15 <i>OD</i>	N15 NCLRF ( $\text{Wm}^{-2}$ )
January	0.92	0.25	0.10	11.4	---	---
February	0.93	0.24	0.10	10.7	0.23	11.4
March	0.86	0.26	0.11	12.3	0.24	11.6
April	0.71	0.28	0.12	16.7	0.25	14.3
May	0.55	0.31	0.11	20.6	0.27	16.6
June	0.44	0.30	0.09	19.7	0.26	16.8
July	0.33	0.31	0.07	21.3	0.28	18.0
August	0.38	0.30	0.08	21.8	0.27	18.9
September	0.45	0.30	0.09	19.8	0.28	17.0
October	0.71	0.31	0.14	19.3	---	---
November	0.84	0.28	0.13	15.7	0.26	13.8
December	0.80	0.28	0.11	14.2	0.26	13.1
Annual	0.66	0.28	0.11	15.8	0.26	15.1

Table 2. N15 & N16 contrail coverage for eastern CONUS, 2001 and estimated combined N15 and N16 CONUS

Month	contrail cover (%)			estimated CONUS
	N15	N16	combined	
January	---	---	---	1.03
February	1.19	0.95	1.07	1.05
March	1.16	0.91	1.03	0.97
April	1.31	0.69	1.00	1.03
May	1.40	0.54	0.97	0.99
June	1.22	0.43	0.83	0.85
July	1.12	0.37	0.75	0.67
August	0.94	0.47	0.71	0.57
September	0.96	0.49	0.73	0.67
October	---	---	---	0.90
November	1.04	0.81	0.93	0.97
December	0.97	0.79	0.88	0.89
Annual	1.17	0.65	0.88	0.88

Table 3. Contrail error analysis results for 3 randomly selected days during each month in 2001. Correction factor (CF) is unitless.

N15	Contrail Coverage (%)			Optical Depth			NCLRF ( $Wm^{-2}$ )		
	remain	del/add	CF	remain	del/add	CF	remain	del/add	CF
April	0.70	0.55/0.08	0.62	0.31	0.23/0.25	1.10	16.6	12.2/13.1	1.10
July	0.57	0.55/0.12	0.62	0.26	0.28/0.16	0.90	18.5	17.8/11.6	0.95
December	0.56	0.42/0.02	0.59	0.28	0.25/0.17	1.03	13.8	11.2/8.2	1.07
mean	0.57	0.48/0.07	0.61	0.28	0.25/0.19	1.01	16.2	14.0/11.7	1.03
.....									
N16									
Feb	0.52	0.49/0.05	0.56	0.20	0.19/0.13	0.99	11.8	8.4/6.9	1.12
April	0.32	0.54/0.18	0.58	0.27	0.30/0.18	0.82	17.3	19.5/10.8	0.90
July	0.15	0.21/0.05	0.56	0.25	0.32/0.17	0.79	18.8	22.7/11.7	0.81
mean	0.31	0.41/0.10	0.57	0.24	0.27/0.17	0.87	14.8	16.5/10.4	0.87

Table 4. Comparison of estimated USA contrail coverage (%).

Month	Current study 2001	Current Study Diurnal correction	Palikonda et al. (1999) 1993-94	Sausen et al. (1998) Theoretical 1992
April	1.00	0.71	2.0	2.0
July	0.67	0.48	1.3	0.5
October	0.90	0.64	1.9	1.9
December	0.89	0.63	2.1	1.6 (Jan)

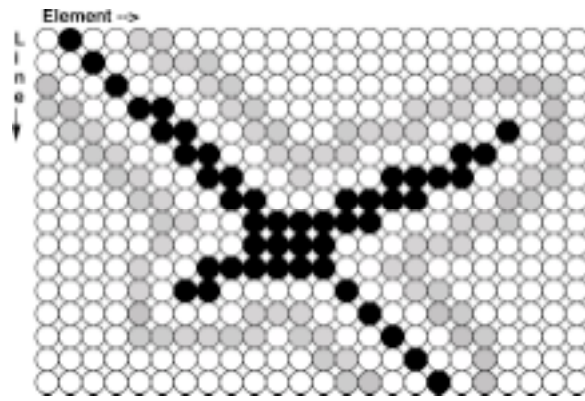


Fig. 1. Schematic of pixels used for computing background radiances. Black - contrail; Gray - background; white - unused.

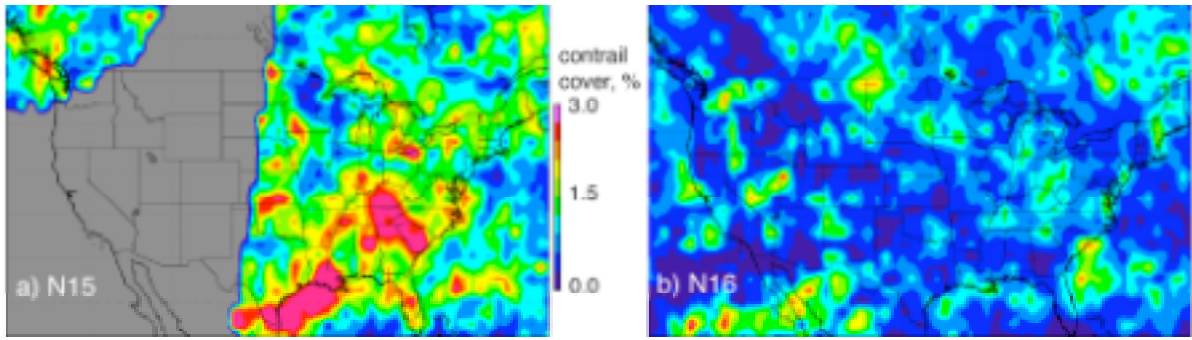


Figure 2. April 2001 daytime contrail coverage

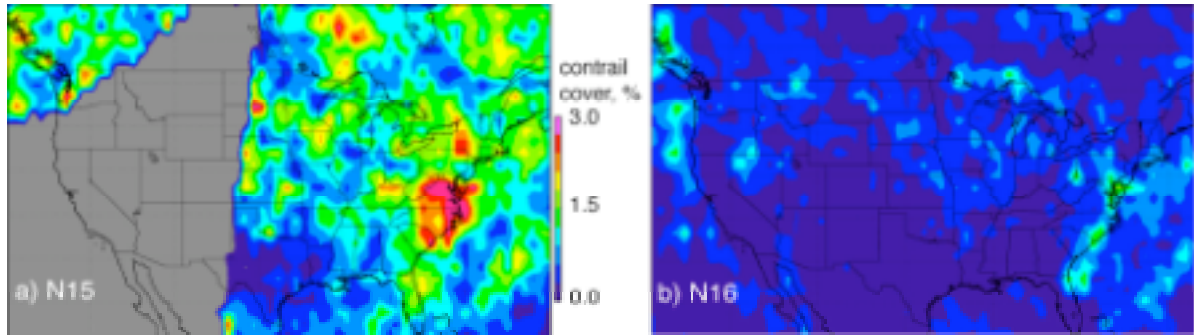


Figure 3. July 2001 daytime contrail coverage

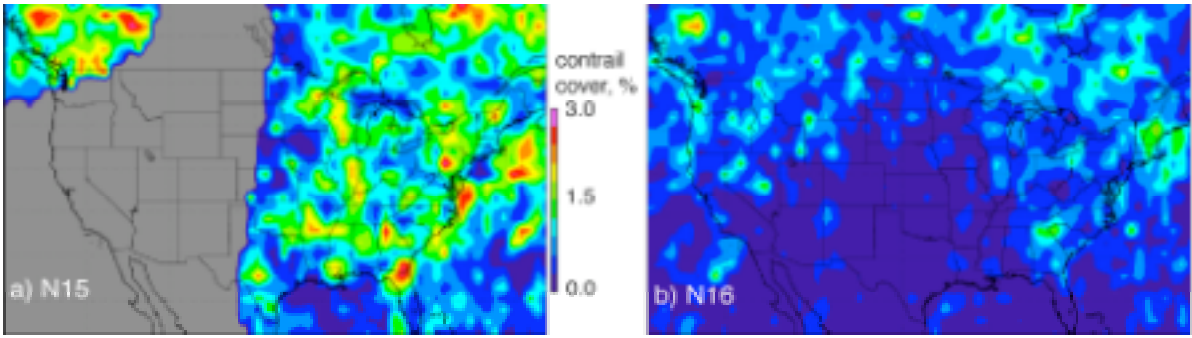


Figure 4. September 2001 daytime contrail coverage.

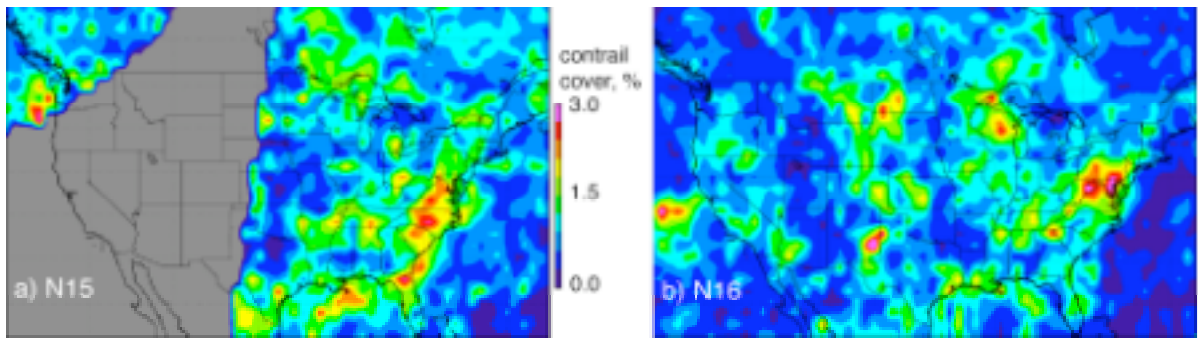


Figure 5. December 2001 daytime contrail coverage.

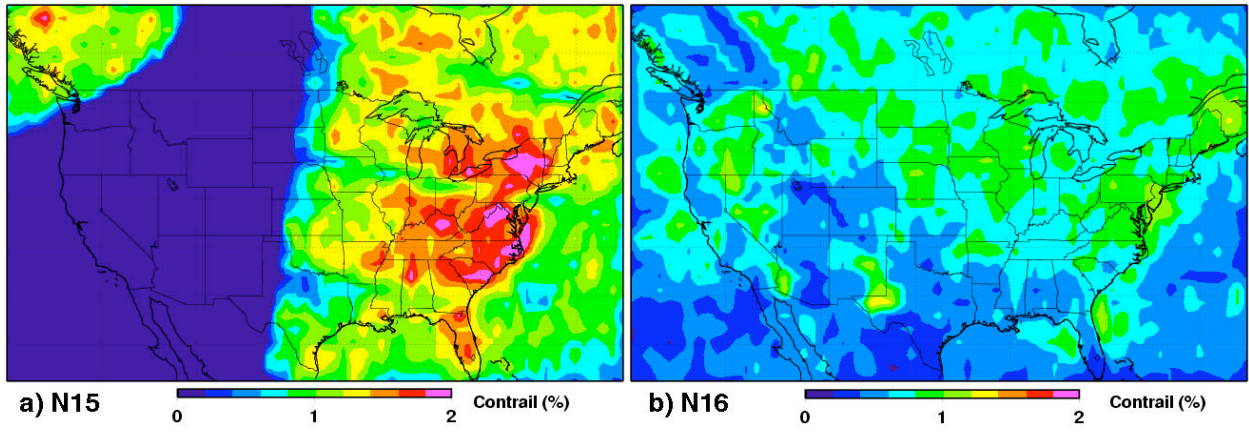


Figure 6. Mean 2001 daytime contrail coverage over USA domain.

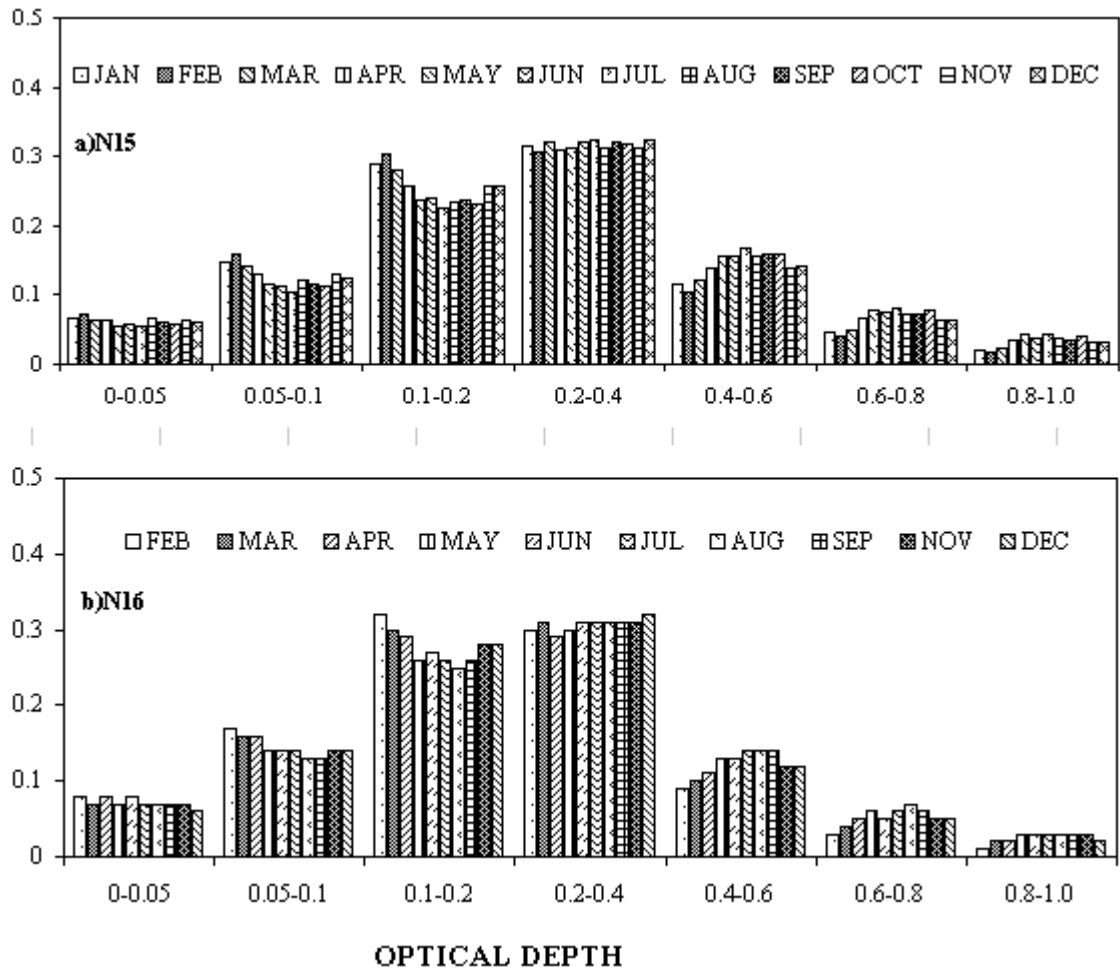


Figure 7. Histogram of daytime contrail optical depths from NOAA-15 and NOAA-16 over USA, 2001.

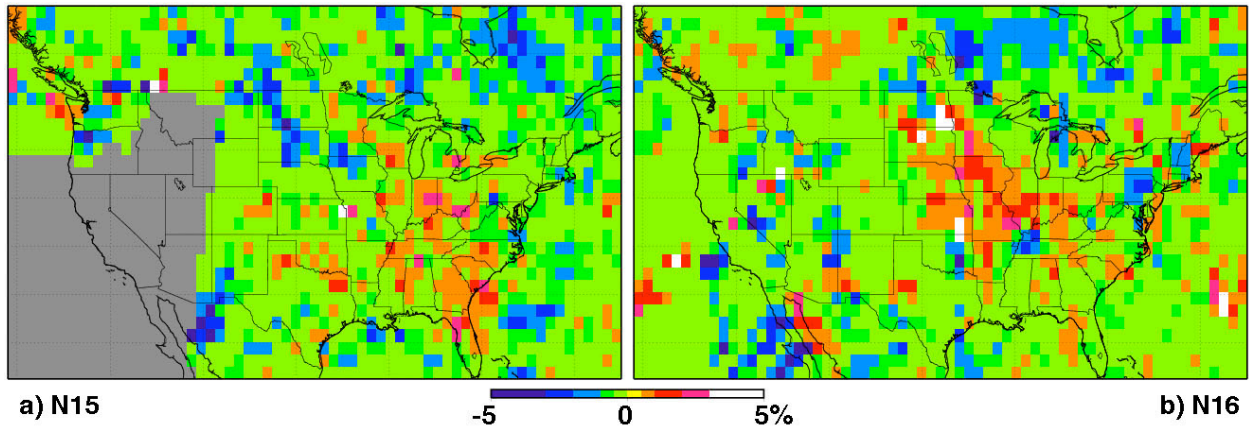


Figure 8. Change in contrail coverage after errors analysis for 9 randomly selected days as described in the text.

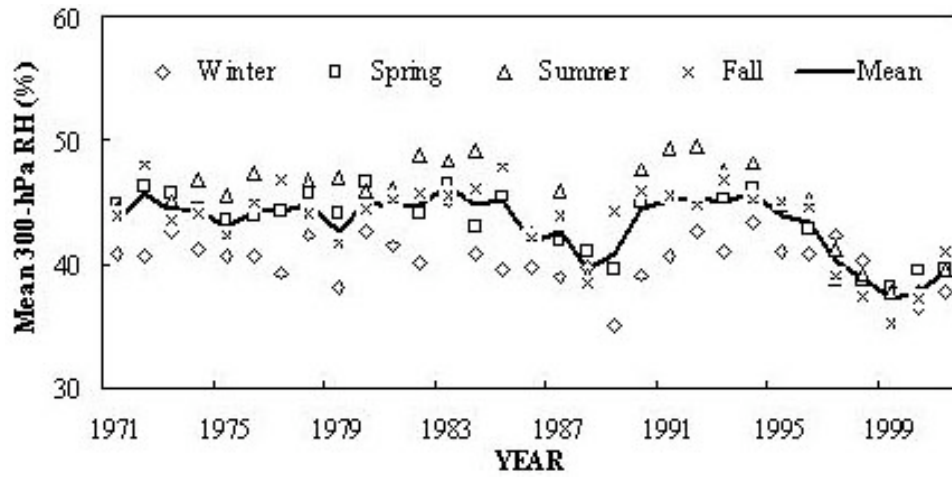


Figure 9. Seasonal and annual mean NCEP RH at 300 hPa over USA.